

From microscopic description to statistical mechanics of Cu-O chain fragments in the high- T_c superconductors $\text{REBa}_2\text{Cu}_3\text{O}_{6+x}$

Hårek Haugerud

University of Oslo, Department of Physics, P.O. Box 1048 - Blindern 0316 Oslo, Norway

Gennadi Uimin*

Institut für Theoretische Physik, Universität zu Köln, D-50937 Köln, Germany

and

*Département de Recherche Fondamentale sur la Matière Condensée, SPSMS/MDN, CENG,
17, rue des Martyrs, F-38054 Grenoble Cedex 9, France*

Walter Selke

Institut für Theoretische Physik B, Technische Hochschule, D-52056 Aachen, Germany

Abstract

The oxygen deficient CuO_x planes of the high- T_c superconductors $\text{REBa}_2\text{Cu}_3\text{O}_{6+x}$ (RE denotes a rare-earth atom or yttrium) are studied. Starting from the Emery model for the Cu-O chain fragments, an *extended* ASYNNNI model is proposed to describe the statistical mechanics of the CuO_x planes. The model is analysed by using Monte Carlo techniques, computing especially the charge transfer to the CuO_2 planes regulating the high- T_c superconductivity, and the concentration of differently coordinated Cu ions. Results are compared to experimental data for various RE cases.

Keywords: REBCO compounds, Cu-O chains, Emery model, ASYNNNI model

I. INTRODUCTION

The high- T_c superconductors $\text{REBa}_2\text{Cu}_3\text{O}_{6+x}$ (REBCO), where RE denotes yttrium or one of the rare-earth atoms Yb, Er, Y, Sm, Nd, or La, have been studied extensively, both theoretically and experimentally. Among others, the impact of the oxygen deficient CuO_x (sometimes called Cu(1)) planes on superconductivity has been investigated. In particular, the charge transfer from the Cu(1) planes to the superconducting CuO_2 (or Cu(2)) planes has been shown to play a crucial role.

The Cu(1) planes consist of linear $\text{Cu}-\text{O}-\cdots-\text{O}-\text{Cu}$ chain fragments (CFs). Each Cu atom is strongly coupled to the two apical oxygen atoms in adjacent Ba-O planes. Depending on the number, l , of neighboring oxygen atoms in a CF, Cu atoms may be $(l+2)$ -fold coordinated. Obviously, a threefold coordinated Cu atom, $\text{Cu}^{(3)}$, is located at the end of a chain fragment; fourfold coordination ($\text{Cu}^{(4)}$) is realized for a copper atom in the CF, while an isolated Cu atom is twofold coordinated, $\text{Cu}^{(2)}$. The concentration of differently coordinated Cu atoms has been determined experimentally by means of NMR-NQR [1,2] and x-ray absorption spectroscopy (XAS) [3,4]. Using the soft XAS method, it is possible to estimate the concentration of oxygen holes in sufficiently long Cu-O chains. For example, for untwinned $\text{YBa}_2\text{Cu}_3\text{O}_7$, it has been found to be about 30% [5].

T_c , the superconducting phase transition temperature, as a function of oxygen content x is known to display the prominent 60 K and 90 K plateaus for $\text{RE} = \text{Yb}$, Y and Er [6], i.e., the compounds of comparatively small RE ionic radii. The analog of the 60 K plateau is less pronounced for $\text{RE} = \text{Gd}$ [7], and the plateaus are practically absent for the REBCO compounds with $\text{RE} = \text{Nd}$ [6,7] and La [8]. The distribution of chain lengths in the CF ensemble allows one to estimate the concentration of holes leaving the chains, n_h , which is usually assumed to be proportional to T_c , unless one is in the underdoping ($n_h < 0.05$) and overdoping ($n_h > 0.25$) regimes. Underdoping corresponds to localization of transferred holes in CuO_2 planes, while overdoping holds near the maximum of $T_c(n_h)$ (see [9] and [10]).

T_c depends not only on x but also on the temperature, T_q , at which the Cu(1) planes have been effectively equilibrated experimentally. T_q is typically the annealing temperature for rapid quenches, or the room temperature, T_R , if the cooling was done slowly; below T_R , the mobility of the oxygen atoms in the CuO_x planes is greatly reduced. Varying T_q up to 350°C in experiments on YBCO, Veal and co-workers [11] showed that the 60 K plateau is sensitive to changes of T_q . In fact, the plateau becomes less pronounced with increasing T_q . A subsequent experiment [12] confirmed these results, and demonstrated that the various annealing temperatures T_q are accompanied by rearrangements in the ensemble of chain fragments. Note, that the temperature considered in our theoretical analysis of the Cu-O chains corresponds to T_q in experiments.

The Cu-O chains in the Cu(1) planes may form differently ordered phases, the orthorhombic, Ortho-I, Ortho-II, and probably Ortho-III (see, for instance, [13–17], as well as the tetragonal phases, which have been identified experimentally. The perfect Ortho-I and Ortho-II structures together with a typical arrangement of oxygen atoms in the tetragonal structure are shown in Figure 1.

The transformation from the semiconducting to the metal state in YBCO is usually ascribed to the tetragonal–orthorhombic transition. The underlying microscopic mechanism seems to be the delocalization of holes in the CuO_2 planes resulting in a change of the oxygen hole chemical potential, which, in turn, influences the structural properties [18].

Some years ago, a lattice-gas model, the asymmetric next-nearest-neighbor Ising (ASYNNNI) model, has been proposed for describing the oxygen ordering in the Cu(1) planes of YBCO [19]. It is based on three effective coupling constants as shown in Figure 2. Two of these couplings, the nearest neighbor oxygen repulsion V_1 (> 0) and the next-nearest neighbor attraction V_2 (< 0) mediated by a copper atom, favor Ortho-I-like configurations. The third coupling, V_3 , the direct interaction between next-nearest oxygen atoms without intermediate Cu atom, is supposed to be repulsive, thereby favoring formation of Ortho-II-like configurations. The phase diagram of the model is sketched in Figure 3. As noted before, when comparing to experiments, the temperature should be interpreted as T_q .

The phase diagram of the ASYNNNI model has been analyzed using various numerical approaches, such as cluster variation methods [20–22], Monte Carlo simulations for static [17,23–25] as well as dynamic properties [26], and transfer-matrix finite-size techniques [27]. Among the approximate analytical approaches, one may mention a low-temperature expansion of the free energy [28] and high-temperature expansions [29,30]. The model allows to reproduce remarkably well the main features of the experimental phase diagram for YBCO. As a note of caution, attention may be drawn, however, to experimental findings providing evidence for a possible discrepancy in the location of the phase boundary of the Ortho-II phase [12,31–33]. According to these experiments, the disordering of the Ortho-II phase, oxygen content x close to 0.5, occurs at about 450 K.

In the ASYNNNI model the internal degrees of freedom of the CFs are ignored, such as the charge and spin distributions. To take them into account, one may start from an appropriate microscopic model of the Cu-O chains and try to map it onto a corresponding lattice-gas model, possibly of ASYNNNI-type. (Microscopic models have been also employed by Aligia [34,35] to explain and predict some superstructures in the Cu(1) planes). Such an approach has been attempted before [36,18], motivated by the suggestion that, in the case of YBCO, the ASYNNNI model may be insufficient to describe phenomena in the part of the phase diagram where short Cu-O chains dominate. For instance, the chemical potential isotherms [37] are reproduced only poorly, whose singularities seem to be important near the tetragonal-to-Ortho-I phase boundary where the average length of the chains does not exceed a few lattice constants. It had been suggested [38–40] to describe the tetragonal phase in YBCO at $x < 0.4$ in terms of a phase separation. In particular, neutron and x-ray data had been interpreted, in the regime of phase separation, as signalling short chains with a herringbone structure. However, subsequently, the superstructure reflections were attributed to a parasitic phase [36]. (Nevertheless, there may be a chance to find herringbone structures or some other regular configurations of the very short chain fragments in LaBCO, but not in YBCO; for possible patterns, see Figure 4. Indeed, it has been shown [41] that those chain fragments are electric quadrupoles, and if they are dominant, then the herringbone structure would be energetically preferred).

The motivation of the present study is to reconsider the ASYNNNI model in view of the new experimental facts. We shall relate that lattice-gas model to a strongly correlated electron model, the Emery model, for the Cu-O chains. This will allow us to reinterpret the crucial coupling V_2 , which will turn out to depend, for instance, on temperature. In addition, a new parameter will be introduced, reflecting the relevance of the shortest chain fragments, i.e. Cu-O-Cu. Using Monte Carlo simulations, properties of the resulting *extended* ASYNNNI model will be computed, based on the statistical ensemble of chain fragments. The main considerations in relating the Emery model to the ASYNNNI model will be presented in the next section, followed by a section in which, based on

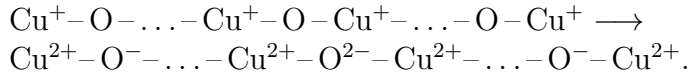
the lattice-gas model, some interesting properties like the temperature dependence of the charge transfer from the Cu-O chains in the Cu(1) planes to the Cu(2) planes for various REBCO compounds as well as the distribution of differently coordinated Cu atoms will be discussed. A short summary will conclude the article.

II. MICROSCOPIC DESCRIPTION

Charge transfer mechanism

Following prior considerations [42], we shall describe briefly a possible charge transfer mechanism for the Cu-O chains in the Cu(1) planes.

Assuming a strong repulsion between neighboring oxygen sites, see Figure 2, linear Cu-O chain fragments are formed with essentially no crossings. In a CF, oxygen and copper atoms form a strongly correlated system due to a strong hybridization of the oxygen $p_x(p_y)$ orbitals with the $d_{z^2-x^2}(d_{z^2-y^2})$ orbitals of the copper atoms. If we ignored the oxidation process, the n oxygen atoms in a CF of composition $\text{Cu}_{n+1}\text{O}_n$ would be neutral, while the $n+1$ Cu atoms would be in the monovalent state, as in the parent compound $\text{YBa}_2\text{Cu}_3\text{O}_6$. In reality, a charge transfer is expected to occur, which may be described formally as a two-step process. The first step corresponds to a charge redistribution in the CF, leading to only one divalent O^{2-} ion in each CF; schematically



The second step involves a charge transfer from the monovalent oxygen ions in a chain fragment to the Cu(2) planes or to other fragments. The resulting CF has the form $\text{Cu}_{n+1}^{2+}\text{O}_m^{2-}\text{O}_{n-m}^-$, where $m-1$ holes have been transferred, assuming that each copper ion remains in the divalent state. It has been shown experimentally [5] that for long chains in YBCO $m/n \approx 0.7$. For short chains, the optimal CF configurations have been estimated [42] to be $\text{Cu}_5^{2+}\text{O}_3^{2-}\text{O}^-$ for $n=4$, $\text{Cu}_4^{2+}\text{O}_2^{2-}\text{O}^-$ for $n=3$ and $\text{Cu}_3^{2+}\text{O}^{2-}\text{O}^-$ (or $\text{Cu}_3^{2+}\text{O}_2^{2-}$) for $n=2$. Accordingly, no hole (one hole) leaves the $n=2$ CF, one hole and two holes leave the $n=3$ and $n=4$ CF, respectively. Generalizing this finding into a simple rule of thumb, one may estimate m to be, for an arbitrarily long chain, $m = \text{nint}(n(m/n)_{\text{opt}})$, where nint denotes the nearest integer. $(m/n)_{\text{opt}}$ is that optimal ratio, which is realized in *long* CFs.

The Emery model

As the starting point for a microscopic description of the Cu-O chains we use the one-dimensional Emery model [43], applied to systems of finite length. The Hamiltonian is

$$\begin{aligned} H = & -t \sum_{\langle r, \rho \rangle} \sum_{\sigma} \left(p_{r\sigma}^{\dagger} d_{\rho\sigma} + d_{\rho\sigma}^{\dagger} p_{r\sigma} \right) + \sum_r (\epsilon_p n_r + U_p n_{r\uparrow} n_{r\downarrow}) + \\ & + \sum_{\rho} (\epsilon_d n_{\rho} + U_d n_{\rho\uparrow} n_{\rho\downarrow}) + U_{\text{end}} \sum_{\tilde{\rho}} n_{\tilde{\rho}} \end{aligned} \quad (1)$$

where the sum runs over the O sites (r) and the Cu sites (ρ) of a *finite* chain, $\langle r, \rho \rangle$ denotes neighboring lattice sites, and $\tilde{\rho}$ refers to the $\text{Cu}^{(3)}$ sites at the chain ends. d_{σ} and p_{σ} (d_{σ}^{\dagger} and p_{σ}^{\dagger}) are annihilation (creation) operators of a hole with spin σ on Cu and O

sites, respectively. n_σ is the hole (spin σ) occupation number and $n = \sum_\sigma n_\sigma$. This model ignores the contribution of the apical oxygen ions to the energy, which, indeed, play a minor role, because they are essentially divalent (cf discussion in [44]).

Because of the quantum origin of alternating Cu-O chains, the hole occupation number on Cu sites is not rigorously equal to 1, as tacitly assumed when the charge transfer mechanism was discussed. This occupation number fluctuates, remaining slightly below 1 (≈ 0.85 , as numerically estimated in [45]). Now, a good quantum number is the number of holes (both, oxygen and copper), say $\nu(n)$ in a CF of length n . Nevertheless, m remains a quantum number, characterizing the hole transfer from a chain. The relation between $m(n)$ and $\nu(n)$ is given by

$$\nu(n) = 2n - (m(n) - 1). \quad (2)$$

There are strongly correlated models, e.g., the Kondo-reduced Emery model (see [42,46]), which allow to treat Cu ions of CFs as divalent, and oxygen ions as monovalent ($n - m$) or divalent (m).

Note that we include in model (1) the shift of the on-site hole energy level, U_{end} , which is due to non-equivalency of $\text{Cu}^{(3)}$ and $\text{Cu}^{(4)}$ ions. There may be alternate ways to take into account the U_{end} -term; for instance Aligia uses a model [34,35] which includes the interaction of charges of neighboring atoms, $\rho(\text{Cu})$ and $r(\text{O})$,

$$U_{\text{pd}} \sum_{\langle r, \rho \rangle} (1 + n_\rho)(-2 + n_r)$$

Our description could be interpreted as a simplified version of the U_{pd} -term, $U_{\text{end}} \approx U_{\text{pd}}(2 - \bar{n}_r)$, where \bar{n}_r denotes the thermal expectation value for the occupancy of an oxygen site.

In the case of RE=Nd or La, the ionic radii of the rare-earth ions are larger than in the other REBCO compounds. Consequently, the interatomic distance is also larger, but the hole hopping amplitude is smaller – in the chains, and in the planes. We shall discuss below why this circumstance may favor short chain fragments, depending on the oxygen hole chemical potential, μ , which varies in the REBCO series.

Free energy

We consider the $\text{Cu}_{n+1}^{2+}\text{O}_m^{2-}\text{O}_{n-m}^-$ chain fragment, described by the Emery model (1). We may determine, say, numerically, its free energy (here and in the following, the free energies are taken per oxygen atom), $f(n; m)$. Indeed, performing statistical averaging with respect to the internal, fermionic, degrees of freedom (m and possible spin arrangements), and disregarding the configurational entropy, the free energy for long chains ($n \gg 1$) has been recently shown to have the form [30]

$$\phi(n) \approx \phi_1 - \frac{\phi_2}{n} - \frac{T}{2n} \ln n. \quad (3)$$

where ϕ_1 and ϕ_2 are coefficients which are given by the energy parameters of the Emery model; ϕ_2 is, approximately, linear in T .

In specifying the parameters of the Emery model, we largely follow Refs. [45,18]. ϵ_d is taken as the reference level. Measuring the other energy parameters in units of t , we set $\epsilon_p = 2$, $U_p = 4$ and $U_d = 8$, similar to the values in the CuO_2 planes of YBCO. The

REBCO compounds are expected to differ mainly in the value of the hopping amplitude t (being approximately $t = 1.35 \text{ eV} \approx 15000 \text{ K}$ for YBCO). As noted before [45,18], the remaining two parameters, the chemical potential μ and U_{end} , play an essential role in favoring long or short chains. μ equilibrates the hole exchange between the two oxygen hole reservoirs, CuO_2 planes and CFs. U_{end} stems from the non-equivalency of the $\text{Cu}^{(3)}$ and $\text{Cu}^{(4)}$ sites ($\epsilon_d + U_{\text{end}}$ denotes the hole level on a $\text{Cu}^{(3)}$ -site). Although U_{end} is positive, as seen from its relation to U_{pd} , its exact value is not known, neither from experiments nor from band-structure calculations.

In YBCO the oxygen atoms of the oxygen deficient planes tend to arrange themselves into long chains at low enough quenching temperatures; probably even at quite low oxygen content. In contrast, in LaBCO long chains are predominant only at $x \sim 1$ [2]. In the REBCO compounds, the various tendencies in the chain lengths are expected to be caused by the various ionic radii of their rare-earth constituents (see Table I). In the model description (1) of those compounds, the crucial parameters are the hopping amplitude t which depends on the RE ionic radius, and the chemical potential which regulates the degree of filling of the 1D O-hole band.

To see whether short or long Cu-O chains are favored, we compute the free energy per oxygen atom as a function of the chain length. If it increases with length, then short chains are more likely, otherwise longer chains are preferred.

For a given set of parameters one may calculate the free energy in the grand canonical ensemble, thus incorporating the chemical potential μ , which governs the concentration of holes in a chain. Following this scheme one needs, in principle, the whole set of energy levels of the Emery model. However, since the temperatures we are dealing with are much lower than the typical electronic energies, which are of order several thousand K, it is sufficient to include the lowest energy levels in the free energy calculations. These levels may be determined by using the Lanczos algorithm [47], as we did in evaluating the free energy of chains with up to $n = 6$ oxygen atoms (plus 7 copper atoms). The detailed procedure for calculating the free energies is described in Appendix A.

III. THE EXTENDED ASYNNNI MODEL

Estimate of effective parameters

The free energy of the chains described by the Emery model, expression (3), corresponds in the standard ASYNNNI model to the energy of a Cu-O chain with n oxygen atoms, neglecting interchain interactions, i.e.

$$\tilde{\phi}(n) = V_2 - \frac{V_2}{n}. \quad (4)$$

A clear difference of $\phi(n)$ and $\tilde{\phi}(n)$ is that $\tilde{\phi}(n)$ decreases monotonically with n at $V_2 < 0$, whereas, if the analogous condition $\phi_2 < 0$ is satisfied, $\phi(n)$ exhibits a minimum at finite, but exponentially large value $n_{\text{opt}} \propto \exp 2\phi_2/T_q$. It is estimated as exceeding a hundred at temperatures below 300° C . Hence, the logarithmic correction in the r.h.s. of Eq.(3) may start playing an important role only at $x \sim 1$.

ϕ_2 in Eq.(3) depends on temperature, while V_2 does not (in both cases, we did not consider the configurational entropy). Accordingly, accepting the Emery model as the more fundamental description for the chain fragments, the ASYNNNI model may be

modified by introducing an effective, *temperature-dependent* coupling V_2 , corresponding to ϕ_2 in the Emery model. The difference in the coefficients ϕ_1 and ϕ_2 may not break the analogy with the ASYNNNI model. In relevant experiments, the CF ensemble is measured at a fixed oxygen content, thus ϕ_1 contributes equally to any realization of CFs and may be rescaled, say, to the value of ϕ_2 .

Note that Eq.(3) holds only for sufficiently long chains. Indeed, for short chain fragments, $\phi(n)$ may show oscillations [18]. To include these subtle features in a statistical description (for example, in a Monte Carlo simulation), one may deal with the free energies of the short chains separately. The largest deviation from the expressions (3) and (4) occurs at $n = 1$. Thence, to incorporate those oscillations in the simplest fashion, we consider an *extended* ASYNNNI model, attributing to the chains with $n = 1$, Cu-O-Cu, an additional energy \tilde{V}_2 . For larger values of n , we keep the parameters of the standard ASYNNNI model. Accordingly, the free energy may be cast in the form

$$\tilde{\phi}(n) = V_2 - \frac{V_2}{n}, \quad n > 1; \quad \tilde{\phi}(1) = \tilde{V}_2. \quad (5)$$

To substantiate Eqs.(3) and (5), we shall now present results of calculations of the free energy for the Emery model of Cu-O chain fragments.

Let us first roughly estimate a realistic value of U_{end} . In Figure 5, the free energy of the Emery model is shown, using units appropriate for YBCO (we have chosen the chemical potential μ at each U_{end} to assure that the concentration of oxygen holes in the *longest* chains we studied is ≈ 0.3). Specifically, the energy parameters are taken in units of $t = 1.35$ eV ≈ 15000 K, so that the temperature range of experimental interest (T_q between 300 K and 1200 K) is between 0.02 and 0.08. Comparing the free energies for long chains to expression Eq. (4) (disregarding, at this stage, \tilde{V}_2) one finds that $U_{\text{end}} = 1$ corresponds to a moderately attractive V_2 , of several hundreds of Kelvin in agreement with the experimentally observed disordering of the Ortho-II phase at about 450 K. Otherwise, for example, for $U_{\text{end}} = 0$ the free energy grows too rapidly with the chain length, corresponding to an effective repulsion V_2 of the order of a few thousands of Kelvin (see also [35]). Increasing U_{end} leads first to a weaker repulsion, and finally an attractive V_2 . For instance, $U_{\text{end}} = 1.5$ would imply a value for V_2 of the order of several thousand K, being a strong effective attraction. Thereby, by tuning U_{end} , one may stabilize either short chain fragments (some realizations at $x \leq 1/2$ are shown in Figure 4) or very long Cu-O chains.

While U_{end} is expected to be essentially a constant for all REBCO compounds, the chemical potential μ may vary, e.g., with the oxygen content x or the RE element. In Figure 6 the free energy per oxygen is shown for several values of the chemical potential at the particular choice $U_{\text{end}} = 1$. With μ increasing, the effective intra-chain interaction V_2 between the oxygen atoms in the Cu-O chains changes from attraction to repulsion. This is happening in a fairly broad range, $\mu = 1.5 - 2.0$, where V_2 goes from a moderately attractive value (~ -0.15) to a moderately repulsive one (~ 0.1). Changing the RE element in the REBCO compounds implies changing μ and hence the intra-chain interaction. As will be discussed later, V_2 varies slowly, remaining ~ -0.1 in the range of relevant values of μ . In fact, \tilde{V}_2 introduces an important competing effect.

In Figure 7 we depict the free energy per oxygen atom versus n for $U_{\text{end}} = 1$ at different temperatures, choosing the chemical potential so that the concentration of oxygen holes is, for long chains, approximately 0.3, as it is the case for YBCO. $\mu \approx 1.6$ is well compatible with that concentration. One may easily see that the lower the (quenching) temperature

T the larger the effective intra-chain oxygen-oxygen attraction will be. In addition, at low T , the free energy shows an oscillatory behavior for small values of n (see, for example, Figure 7 at $T = 0.02$). Such oscillations are maximal at $T = 0$ (see also Figure 1 in [18]). It is obvious from Figure 7 that the fitting of the free energy to that of the standard ASYNNNI model, Eq.(4), is unsatisfactory even in the high temperature region. The $n = 1$ case has to be fitted separately, defining \tilde{V}_2 in the extended ASYNNNI model, Eq.(5). It should be emphasized, that the effective parameters of the hereby defined *extended* ASYNNNI model, V_2 and \tilde{V}_2 , depend not only on the temperature, but also on U_{end} . In addition, they depend on a specific filling of the 1D oxygen hole band, i.e. μ .

The other two couplings of the full ASYNNNI model, V_1 and V_3 , are of predominantly electrostatic origin, and may be supposed to be constant. Of course, their values do not follow from the Emery model. (At this point, attention may be drawn to another attempt to determine parameters of the (standard) ASYNNNI model from first-principles, based, in that case, on linear muffin-tin-orbital calculations for YBCO [48]. In that analysis, only ground state properties have been considered, leading to constant couplings V_1 , V_2 , and V_3 .)

In Figure 7, also least-square fits of the free energy for the Emery model to the ansatz, Eq. (5), defining the extended ASYNNNI model are shown, at several temperatures. From such fits one may determine V_2 and \tilde{V}_2 as function of temperature. Examples are shown in Figures 8 and 9 for a few values of U_{end} around $U_{\text{end}} = 1$, presuming a fixed hole concentration of 0.3 in the longest chains. It is evident from Figure 8 that V_2 displays a pronounced linear dependence on T (cf, Eq.(3), where ϕ_2 is also linear in T), and V_2 is practically linear in U_{end} at a given temperature.

To fix U_{end} , one may compare results on the extended ASYNNNI model to experiments. A possible procedure will be demonstrated now for YBCO. There we estimate U_{end} by locating the disordering transition of the Ortho-II phase of $\text{YBa}_2\text{Cu}_3\text{O}_{6+x}$ with $x = 0.5$, known to occur experimentally at about 450 K [12,31–33]. That transition temperature is found to depend rather sensitively on the choice of U_{end} , and hence V_2 and \tilde{V}_2 in the framework of the extended ASYNNNI model. The lattice gas model is analysed by using standard Monte Carlo (MC) techniques.

To simulate the extended ASYNNNI model, one first has to specify the couplings V_1 and V_3 . Different values have been proposed and studied for the conventional ASYNNNI model [19,23,22]. Here we adopt values which have been argued to reproduce the experimental structural phase diagram of YBCO fairly well [24,25], namely, in terms of V_2 ,

$$V_1 = -2.86 \cdot V_2 \quad (6)$$

$$V_3 = -0.46 \cdot V_2 \quad (7)$$

As discussed above, V_2 is expected to depend on temperature much more strongly than V_1 and V_3 . Thence, in fixing V_1 and V_3 , we choose the value of V_2 at the Ortho-II disordering temperature, $T_{\text{II}} \approx 0.03$ (note that we checked, by simulations, that choosing the room temperature T_R , instead of T_{II} , leads to rather minor changes of V_1 and V_3 , of a few percent, and affects the estimate for U_{end} only mildly).

Simulations at T_{II} for different values of U_{end} (and tuning μ to reproduce the hole concentration for the longest chains), which determine $V_2(T_{\text{II}}; U_{\text{end}})$ and $\tilde{V}_2(T_{\text{II}}; U_{\text{end}})$ have been performed. The order parameter m_{II} [23,25] of the Ortho-II phase is found to drop abruptly at $U_{\text{end}} = 1.02$, see Figure 10. From Figures 8 and 9, one obtains $V_2(T_{\text{II}}) \approx -0.12$ and $\tilde{V}_2(T_{\text{II}}) \approx -0.09$. Summarizing, we have finally estimated, for YBCO, $U_{\text{end}} = 1.02$

and $\mu = 1.59$ from the experimental values of T_H and the hole concentration for long chains.

In substituting yttrium by another RE element, the chemical potential will be changed. This, in turn, will lead to different values of the effective parameters in the ASYNNNI model. Results of pertinent calculations are depicted in Figure 11, taking $U_{\text{end}} = 1.02$. By changing μ in between 1.55 and 1.70, one induces only mild changes in V_2 , in between -0.15 and -0.1. More importantly, we observe in that range a crossover in the tendency to form short or long Cu-O chains. Obviously, that tendency follows from the fact whether \tilde{V}_2 is smaller than V_2 , or vice versa. At $\mu = 1.59$ (characteristic for YBCO), the long chains are favored; at $\mu \approx 1.65$, a compensation holds. At larger values of the chemical potential, short chains will be preferred.

Accordingly, for each REBCO compound, one may predict the preference for short or long chains from the value of μ . Although the chemical potential is not precisely known for the various RE cases, one may safely assume that it increases with the ionic radius. As shown in table I, these radii vary appreciably. For instance, they are larger for Nd and La than for Y.

A microscopic description for estimating μ should invoke the structure of the oxygen hole bands of the chain fragments (1D) as well as of the Cu(2) planes (2D). It has been assumed in [18] that the 1D oxygen hole band is lower than the 2D band, with an overlap, as shown schematically in Figure 12, where μ is above the bottom of the 2D hole band. Despite a potentially significant charge transfer from chains (i.e. $\overline{m(n)} - 1$ from each CF of length n), such a band structure is no contradiction. In fact, at small oxygen content x , shorter CFs are preferred, the charge transfer gets effectively suppressed. The holes transferred from chains become partly localized on the impurity levels and partly 2D carriers, with a rather low, semiconducting, concentration. In the metallic state the chemical potential intersects the 2D band; a sufficiently large hole transfer from chains to planes causes an electrostatic shift of the levels, and the 1D band raises with respect to the 2D band. Based on such a description, the transformation from the semiconducting to the metallic state, by changing the oxygen content x , can be qualitatively described [18,49].

In principle, one could estimate the variation of μ with x from a self-consistent scheme which would be very tedious, based upon experimental data which have not been established reliably, so far. In the following analysis, we shall, however, assume that the chemical potential is independent of x . This will be sufficient to reproduce the main trends resulting from the change in μ in the REBCO series. To describe the corresponding thermal properties of the chain fragments, we shall investigate the extended ASYNNNI model, with the parameters \tilde{V}_2 and V_2 changing with the chemical potential. For V_1 and V_3 , we shall always take the values for YBCO, see above. Because they are associated with Coulomb forces on small distances, they are expected to vary only slightly, by a few percents, when substituting Y by, say, Nd or La. As we checked in simulations, such a variation will not affect the conclusions. The results of the Monte Carlo study will be compared to experimental findings for LaBCO and NdBCO [1,2].

Monte Carlo simulations, Comparison with experiments, Discussions

The simulations of the extended ASYNNNI model describing REBCO compounds have been performed for systems with $L \times L$ Cu sites, imposing full periodic boundary

conditions. Usually, L was taken to be 40; to estimate the role of finite size effects, a few runs were done with larger lattices. We employed Kawasaki dynamics, keeping the oxygen content x constant during a simulation, and choosing the initial and final site of an oxygen atom randomly. The new site, if empty, is accepted with a probability given by the Boltzmann factor of the change in energy of that possible move. An updating scheme which restricts the hopping of the oxygen atoms to neighboring lattice sites would be more realistic in mimicing dynamical processes, but slower. Because we are here only interested in equilibrium properties, we employed the faster algorithm.

By varying the oxygen content x and the temperature T , the structural phase diagram may be determined. Figure 13 depicts the phase diagram for the case of YBCO, using the values of the effective parameters discussed above. The phase boundaries have been estimated from the behavior of the order parameters of the various phases and the positions of the maxima in the specific heat, as before [23]. The topology of the phase diagram is similar to that obtained for the standard ASYNNNI model in prior computations, e.g. [23,24], including the Ortho-I, Ortho-II, and tetragonal phases. Perhaps most notably, the maximal phase transition temperature of the Ortho-II phase is, however, somewhat reduced, in accordance with the experimental findings.

By analysing Monte Carlo equilibrium configurations one may easily identify the Cu-O chain fragments and hence determine, for instance, the thermally averaged concentration of differently coordinated Cu ions. In Figure 14 the concentration of $\text{Cu}^{(2)}$ ions, c_2 , is shown as a function of the oxygen content for various temperatures, in the YBCO case. While at high temperatures c_2 decreases monotonically with increasing oxygen content, one finds a non-monotonic or plateau-like behavior when lowering the temperature, so that one may encounter the Ortho-II phase. Obviously, in the perfect Ortho-II structure, at $x = 0.5$ and sufficiently low temperatures, half of the Cu atoms belong to the perfect Cu-O chains extending throughout the lattice and half of them are in oxygen-free rows, see Figure 1(c). Accordingly, the concentration of $\text{Cu}^{(2)}$ ions in such an ideal configuration is 0.5. Experimental results of XAS measurements at low and high temperatures [4] are included in Figure 14. Agreement between experimental data and theoretical curves is quite satisfactory, except for the point at $x \approx 0.39$, low T_q , which may, indeed, have been determined inaccurately in the experiment. The behavior of c_2 versus x at $T = 450$ K also agrees rather well with the experimental results using NMR-NQR [1,2]. The concentrations of $\text{Cu}^{(2)}$, $\text{Cu}^{(3)}$ and $\text{Cu}^{(4)}$ (c_2 , c_3 , and c_4) obtained from the MC simulations at $T = 450$ K in the case of YBCO are shown in Figure 15, together with experimental data (their accuracy has not been mentioned) [2]. A few experimental points deviate clearly from the theoretical curves. Note, that the experimental data of [2] plotted in Figure 15 obey well the sum rule

$$c_2 + c_3 + c_4 = 1 \quad (8)$$

This identity assumes that all Cu ions in the Cu(1) planes can be identified as $\text{Cu}^{(2)}$, $\text{Cu}^{(3)}$ or $\text{Cu}^{(4)}$. With that assumption, a second sum rule is evident

$$c_3 + 2c_4 = 2x. \quad (9)$$

These two sum rules allow to express two of the concentrations, say, c_3 and c_4 , by the remaining one, c_2 , and the oxygen content x ; for instance,

$$c_3 = 2 - 2x - 2c_2, \quad c_4 = 2x - 1 + c_2.$$

The concentrations are allowed to vary in the range defined by the following inequalities,

$$\begin{aligned} 0 \leq x \leq 1/2 &\longrightarrow 1 - 2x \leq c_2 \leq 1 - x, \quad 0 \leq c_3 \leq 2x, \quad 0 \leq c_4 \leq x; \\ 1/2 \leq x \leq 1 &\longrightarrow 0 \leq c_2 \leq 1 - x, \quad 0 \leq c_3 \leq 2 - 2x, \quad 2x - 1 \leq c_4 \leq x. \end{aligned} \quad (10)$$

A few points of the experimental set disagree significantly with (9), several points are beyond the limits defined by (10). Note that there is an uncertainty, reaching up to 0.1 according to [2], in determining the oxygen content in the range $0.3 < x < 0.4$ (probably, in the region of phase separation).

As mentioned above two concentrations can be determined by the remaining third concentration. Taking the latter one as c_2 for $x < 0.5$, c_3 for $0.5 \leq x < 0.7$, c_4 for $0.7 < x \leq 0.8$, and again c_2 for $0.8 < x$ (c_4 would be beyond the limit of the inequality), we can fit nicely the revised set of experimental points to theoretical curves in Figure 15.

Similar measurements on the concentrations of differently coordinated Cu ions have been reported for $\text{NdBa}_2\text{Cu}_3\text{O}_{6+x}$ (NdBCO) and $\text{LaBa}_2\text{Cu}_3\text{O}_{6+x}$ (LaBCO) [2]. As argued above, we propose that the effect of the increase of the ionic radius in Nd and La compounds can be incorporated into the microscopic model by an increase in the chemical potential, leading to modified effective parameters in the extended ASYNNNI model. Although μ is expected to depend on the oxygen content x for each REBCO compound, we consider a constant μ for a given RE, for reasons stated before. This simplification seems to be justified in order to detect the main trends. Indeed, when increasing μ from 1.59, for YBCO, to 1.62 and 1.66, for NdBCO and LaBCO, respectively, the simulated data on c_2 , c_3 , and c_4 agree rather well with the experimental results, see figures 16 and 17. For NdBCO we can use c_3 for determining the other concentrations in the range $0.5 < x < 0.7$, as in the YBCO-case. For LaBCO, c_3 and c_4 have not been accessible for direct measurements in the range $0.5 < x$; in this case c_2 plays the determining role.

There may be also five- and sixfold coordinated Cu ions in Cu(1) planes, due to a crossing of perpendicular chain fragments. For example, $\text{Cu}^{(5)}$ would appear, if an oxygen atom formed a 90° configuration with two other oxygen atoms (all three are supposed to be adjacent to the same Cu atom). The energy loss due to a $\text{Cu}^{(5)}$ ($\text{Cu}^{(6)}$) ion would be $2V_1$ ($4V_1$). From the simulations, the concentration of such ions is seen to be very small for all oxygen contents x . A kink in a CF would be energetically somewhat more favorable, albeit being still rather costly, V_1 . At the kink, a fourfold coordinated Cu ion occurs, although it differs from the conventional $\text{Cu}^{(4)}$ ion. Such a kink configuration cannot easily be described by the Emery model.

Another important quantity related to the chain fragments of the oxygen deficient Cu(1) planes, is the charge (hole) transfer, n_h , to the CuO_2 planes. It depends on the chemical potential as well as on other external parameters such as x and T_q . $\nu_h(n)$, the expectation number of holes (thermal averaging) leaving a CF of length n , should be $\overline{m(n)} - 1$ (see Figure 18, showing a rather non-trivial dependence on n); it is associated with the expectation number of oxygen and copper holes $\overline{\nu(n)}$ through (2). For long CFs in YBCO, one has $\overline{m(n)}/n \approx 0.7$; but for short chain fragments, it may differ significantly. The average concentration of oxygen holes transferred from the chains, the charge transfer n_h , may be approximated as, see [23],

$$n_h(\mu; x; T_q) = \frac{1}{L^2} \sum_{n=1}^L \frac{\overline{m(n)} - 1}{2} \langle N_{\text{CF}}(n) \rangle, \quad (11)$$

where $\langle N_{\text{CF}}(n) \rangle$ is the average number of CFs of length n . The factor of $1/2$ appears, because holes from one Cu(1) plane are supplied to two Cu(2) planes.

Note that one can calculate the number of holes $\nu(n)$ in the framework of the Emery model, at least for fairly short chains, see Appendix A, which may then be extrapolated to longer chains.

Figure 19 shows the charge transfer versus oxygen content for a set of equidistant temperatures, obtained from simulating the extended ASYNNNI model for the YBCO case. One observes that below $x \approx 0.25$ the charge transfer to CuO_2 planes is extremely small. In this regime, in the tetragonal phase, short chain fragments dominate, contributing much less to the charge transfer than the long chains. The preference for short chains could be reduced by going to very low (quenching) temperatures which, however, are usually not accessible experimentally (recall that T_q is bounded by T_R from below). The tetragonal phase is still semiconducting, and the holes are mainly localized in CuO_2 planes in the vicinity of the CF from which they originated. The formation of longer CFs leads to a significant increase of the hole transfer, giving rise to the semiconducting-to-metal transformation.

The charge transfer displays a plateau-like behavior near $x = 0.5$, reflecting the well-known 60 K plateau in the transition temperature to the superconducting phase in YBCO at that oxygen content. This aspect has been discussed in quite a few publications before. In many experiments the close relationship between the superconducting transition temperature T_c and n_h has been found [50,51]. For instance, T_c was argued to be linear [52,53] or quadratic in n_h [54,55]. In both cases, the plateau in T_c would correspond to one in n_h . A second, so-called 90 K plateau in T_c versus x occurs at $x > 0.8$, where n_h increases monotonically, while T_c remains almost constant. Overdoping is believed to be responsible for that plateau [9,54]: T_c practically saturates when n_h becomes larger than the optimal hole concentration ($\approx 0.2 - 0.25$).

In Figure 20 the charge transfer n_h versus oxygen content x is depicted at $T = 450$ K for three values of the chemical potential, mimicing, as before, YBCO, NdBCO, and LaBCO, i.e. $\mu = 1.59, 1.62$ and 1.66 . One readily sees, in accordance with the experiments, that the low-temperature plateau in T_c versus x is expected to be much less pronounced in NdBCO [7,6] and absent in LaBCO [8]. In that figure, we also included Monte Carlo data for $\mu = 1.56$, mimicing a REBCO compound where the rare earth ions would be even smaller than yttrium, like YbBCO (see table I). Indeed, it was shown experimentally [6] that the 60 K plateau in YbBCO is even more manifest than in YBCO, in accordance with the MC data.

MC simulations allow to compute easily the average length of Cu-O chain fragments, ℓ . Results are displayed in Figure 21. ℓ is given by the ratio (total length of CFs)/(total number of CFs). The numerator is identical with the number of oxygen ions, while the denominator is, neglecting kinks and crossings of CFs, one half of the $\text{Cu}^{(3)}$ atoms. Thence, one would obtain $\ell = 2x/c_3$. That formula has been used in [2], to express the experimental findings for c_3 for YBCO, NdBCO, and LaBCO in terms of ℓ . However, care is needed in doing that. In Figure 21, we compare Monte Carlo results for ℓ invoking the approximate formula to those using the correct expression for the average chain length. Indeed, the overall agreement is fair, but there are obvious differences near $x \sim 1$.

IV. SUMMARY

The present paper has been motivated, *first*, by recent experimental data on Cu-O chain fragments [2], and, *second*, by the wish of elaborating and concretizing the idea to

relate a microscopic description of those fragments to a statistical analysis, i.e. to relate the quantum mechanics of individual chains to the statistical mechanics of their ensembles [18]. Our main considerations and findings may be summarized as follows.

- We consider the Emery model, which belongs to the family of strongly correlated fermionic (hole) models, incorporating into it the effect of chain ends (U_{end} -term). We assume that the lowest, Cu-like, band is completely filled, whereas the intermediate, O-like, band is partly occupied. The occupancy of the latter band is regulated by the chemical potential μ , which determines the equilibrium of the oxygen hole reservoirs in the CuO_2 planes and CFs.
- In accordance with experimental results, the chemical potential level is assumed to be located in the 1D oxygen hole band of the Cu-O chain fragments. The oxygen hole concentration in long CFs is determined by the chemical potential μ .
- The oxygen hole number in a CF follows from the number of holes leaving the chain. There is essentially no charge transfer from short CFs of lengths $n = 1$ and 2 . This explains the predominance of fairly short CFs in the semiconducting state of the REBCO compounds.
- The "semiconductor-metal" transformation is governed by the dependence of the chemical potential on the oxygen content x . Analysis of finite chains by means of the Emery model shows that CFs of minimal length occur less often when μ decreases. This is expected to be accompanied by an increasing number of holes transferred from chains to planes. Coulomb forces lead to the lowering of μ , which favors longer CFs, giving rise to an additional charge transfer, etc.
- In our analysis, the REBCO compounds have been characterised by different, but fixed values of μ . However, in reality, with x increasing, μ is believed to decrease proportionally to n_h , i.e. the hole doping of the CuO_2 planes. Using Figure 11, these changes of μ could be incorporated into the calculations.
- An important role in the Emery model is played by U_{end} ; the energy loss stemming from the ends of a CF determines the effective attraction or repulsion between the oxygen atoms in CFs. In fact, ignoring this term would result in a very strong O-O repulsion in the chains (of the order of several hundreds meV in the case of YBCO, where the concentration of oxygen holes in long CFs is about 0.3). Experimental data allow one to estimate U_{end} to be ≈ 1 in units of the hopping term t of the Emery model.
- The free energy of the Emery model has been calculated for individual CFs, characterized by their length n , as a function of the chemical potential μ , U_{end} , and the temperature T . For specific REBCO compounds, μ and U_{end} can be fixed using experimental data, e.g., for the oxygen hole concentration and the disordering temperature of the Ortho-II phase. By comparison of the free energy, the values of the parameters of an *extended* ASYNNNI model can then be estimated. In the framework of that model, the structural phase diagrams of the REBCO compounds can be conveniently studied, using, for instance, Monte Carlo simulations.
- The larger the ionic radius of the REBCO compound the higher the chemical potential, and the shorter the Cu-O chain fragments.

- Analysing the extended ASYNNNI model for various RE constituents, we also computed macroscopic properties such as the concentration of differently coordinated Cu ions and the charge transfer from the chain fragments.

In conclusion, the theoretical approach presented in this paper (start from microscopic calculations, identify effective parameters of a statistical model as well as, based on experimental results, their values, and finally perform simulations), allows to reproduce main trends in the statistical properties of Cu-O chain fragments throughout the various RE-BCO compounds. Refinements and extensions, based on additional experimental data, are possible.

Acknowledgement

We should like to thank H. Lütgemeier for informing us about his experimental results. Financial support by the Russian Foundation for Basic Research, the Research Council of Norway (Programme for Supercomputing), and by INTAS (Project 93-211) is gratefully acknowledged.

APPENDIX A: THE FREE ENERGY CALCULATION FOR CHAIN FRAGMENTS

The Hamiltonian of the Emery model for a CF, characterized by n and m , deals with $\nu = 2n + 1 - m$ fermions which are spin-1/2 holes. Positive integers m (> 1) describe the charge transfer from a CF. The eigenstates of this Hamiltonian can be easily divided into blocks which correspond to different numbers ν ($\nu = 0, 1, \dots, 2(2n+1)$) and, at given ν , to different total spin projections ($S_z = -\nu/2, -\nu/2 + 1, \dots, \nu/2$). Any block can be further subdivided into two blocks which consist of either symmetric or antisymmetric states with respect to the central Cu atom of a CF. The size of actual blocks grows fastly with n : CFs with $n = 6$ oxygen atoms, plus 7 copper atoms, are still accessible for calculations of a substantial number of the low lying energy levels.

Our conjecture is that the CF properties, including the concentration of holes, depend on the chemical potential μ which, in turn, is a function of the hole doping. Thus, we must calculate the grand canonical partition function:

$$\Xi_n(T, \mu) = \sum_{\nu=0}^{2(2n+1)} \sum_{S_z=-\nu/2}^{\nu/2} \sum_i e^{-[E_i(\nu, S_z) - \mu\nu]/T}, \quad (\text{A1})$$

where i runs over all the states within the block at given ν and S_z . The temperatures of interest do not exceed 1200 K, which is low on the energy scale of the model (1). Indeed, e.g., including one thousand low lying energy levels at $n = 6$, we can properly evaluate the partition function (doubling the number of low lying states, one does not change the free energy significantly).

According to [5], one has $\bar{m}/n \approx 0.7$, provided the copper hole occupation number is equal to one. We incorporate this fact, demanding the average total hole number $\bar{\nu} = 7 + 6 \cdot 0.3 \approx 8.8$ for the longest chains ($n = 6$ oxygen and seven copper atoms), analysed using the Lanczos algorithm [47]. Thus, $\bar{\nu}$ is defined as

$$\bar{\nu} = \frac{1}{\Xi_n} \sum_{\nu=0}^{2(2n+1)} \sum_{S_z=-\nu/2}^{\nu/2} \sum_i \nu e^{-[E_i(\nu, S_z) - \mu\nu]/kT} \quad (\text{A2})$$

and $\mu(T)$ is then numerically determined from the constraint $\bar{\nu} = 8.8$ for $n = 6$.

In the framework of the Lanczos algorithm [47], applied to a block of the states $\{\nu, S_z\}$, we can find, say, the M lowest eigenvalues. $4M$ iterations should guarantee convergence of M eigenfunctions. There may be a problem with the Lanczos algorithm: it fails to distinguish two or more degenerate eigenvalues. However, this is not a serious problem in our case, since the accidental degeneracy occurs only rarely in the Emery model. This has been checked by calculating exactly the eigenvalues for CFs up to $n = 3$.

REFERENCES

- * On leave from Landau Institute for Theoretical Physics, Chernogolovka, Moscow District 142432, Russia.
- [1] H. Lütgemeier, I. Heinmaa, D. Wagener, and S.M. Hosseini, in "Phase Separation in Cuprate Superconductors", Proc. of the International Workshop in Cottbus 1993, p. 225. Edited by E. Sigmund and K.A. Müller, (Springer Verlag 1994).
 - [2] H. Lütgemeier, S. Schmenn, P. Meuffels, O. Storz, R. Schöllhorn, Ch. Niedermayer, I. Heinmaa, and Yu. Baikov, *Physica C* **267**, 191 (1996).
 - [3] J.M. Tranquada, S.M. Heald, A.R. Moodenbaugh, and Y. Xu, *Phys.Rev. B* **38**, 8893 (1988).
 - [4] H. Tolentino, F. Baudelet, A. Fontaine, T. Gourieux, G. Krill, J.Y. Henry, and J. Rossat-Mignod, *Physica C* **192**, 115 (1992).
 - [5] A. Krol, Z.H. Ming, Y.H. Kao, N. Nücker, G. Roth, J. Fink, G.C. Smith, K.T. Park, J. Yu, A.J. Freeman, A. Erband, G. Müller-Vogt, J. Karpinski, E. Kaldis, and K. Schönmann, *Phys.Rev. B* **45**, 2581 (1992).
 - [6] M. Buchgeister, W. Hiller, S.M. Hosseini, K. Kopitzki, and D. Wagener in "Physics and Material Science of High Temperature Superconductors", p. 319. Edited by R. Kossowsky, S. Methfessel and D. Wohlleben (Kluwer Academic Publishers, The Netherlands, 1990).
 - [7] B.W. Veal, A.P. Paulikas, J.W. Downey, H. Claus, K. Vandervoort, G. Tomblins, H. Shi, M. Jensen, and L. Morss, *Physica C* **162-164**, 97 (1989).
 - [8] T.B. Lindemer, B.C. Chakoumakos, E.D. Specht, R.K. Williams, and Y.J. Chen, *Physica C* **231**, 80 (1994).
 - [9] Y. Tobura, in "Physics of High-Temperature Superconductors", Springer Series in Solid-State Sciences, V. 106, p. 191. Edited by S. Maekawa and M. Sato (Springer-Verlag, 1992).
 - [10] The high- T_c superconductors $\text{La}_{2-x}\text{Sr}_x\text{CuO}_4$ for which $T_c(x)$ exhibits a maximum in $T_c(x)$ at $x \approx 0.15 - 0.2$.
 - [11] H. Claus, S. Yang, A.P. Paulikas, J.W. Downey, and B.W. Veal, *Physica C* **171**, 205 (1990).
 - [12] G.V. Uimin, V.F. Gantmakher, A.M. Neminsky, L.A. Novomlinsky, D.V. Shovkun, and P. Brüll, *Physica C* **192**, 481 (1992).
 - [13] Th. Zeiske, R. Sonntag, D. Hohlwein, N.H. Andersen, and Th. Wolf, *Nature* **353**, 542 (1991).
 - [14] P. Burlet, V.P. Plakhty, C. Martin, and J.Y. Henry, *Phys.Lett. A* **167**, 401 (1992).
 - [15] V. Plakhty, A. Stratilatov, Yu. Chernenkov, V. Fedorov, S.K. Sinha, C.K. Loong, B. Gaulin, M. Vlasov, and S. Moshkin, *Solid State Commun.* **84**, 639 (1992).
 - [16] D. Hohlwein, in Proc. of the International School of Crystallography in Erice 1993, edited by E. Kaldis, (Kluwer, Dordrecht 1994).
 - [17] H.F. Poulsen, N.H. Andersen, J.V. Andersen, H. Bohr, and O.G. Mouritsen, *Nature* **343**, 544 (1990).
 - [18] P. Gawiec, D. R. Grempel, G. Uimin, and J. Zittartz, *Phys.Rev. B* **53**, 5880 (1996).
 - [19] D. de Fontaine, L.T. Wille, and S.C. Moss, *Phys.Rev. B* **36**, 5709 (1987).
 - [20] L.T. Wille and D. de Fontaine, *Phys.Rev. B* **37**, 2227 (1988).
 - [21] L.T. Wille, A. Berera, and D. de Fontaine, *Phys.Rev.Lett.* **60**, 1065 (1988); R. Kikuchi and J.S. Choi, *Physica C* **160**, 347 (1989).
 - [22] G. Ceder, M. Asta, W. C. Carter, M. Kraitichman, D. de Fontaine, M. E. Mann and M. Sluiter, *Phys.Rev. B* **41**, 8698 (1990).

- [23] W. Selke and G. Uimin, *Physica C* **214**, 37 (1993).
- [24] T. Fiig, J.V. Andersen, N.H. Andersen, P.A. Lindgård, O.G. Mouritsen, and H.F. Poulsen, *Physica C* **217**, 34 (1993).
- [25] T. Fiig, N.H. Andersen, J. Berlin, and P.A. Lindgård, *Phys.Rev. B* **51**, 12246 (1995).
- [26] J.V. Andersen, H. Bohr, and O.G. Mouritsen, *Phys.Rev. B* **42**, 283 (1990); H.F. Poulsen, N.H. Andersen, J.V. Andersen, H. Bohr, and O.G. Mouritsen, *Phys.Rev.Lett.* **66**, 465 (1991).
- [27] N.C. Bartelt, T.L. Einstein, and L.T. Wille, *Phys.Rev. B* **40**, 10759 (1989); T. Aukrust, M.A. Novotny, P.A. Rikvold, and D.P. Landau, *Phys.Rev. B* **41**, 8772 (1990); D.K. Hilton, B.M. Gorman, P.A. Rikvold, and M.A. Novotny, *Phys.Rev. B* **46**, 381 (1992); D.J. Liu, T.L. Einstein, P.A. Sterne, and L.T. Wille, *Phys.Rev. B* **52**, 9784 (1995).
- [28] J. Oitmaa, Y. Jie and L.T. Wille, *J.Phys.: Condens. Matter* **5**, 4161 (1993).
- [29] G. Uimin, *Int.J.Mod.Phys. B* **6**, 2291 (1992).
- [30] G. Uimin, *Phys.Rev. B* **50**, 9531 (1994).
- [31] S. Yang, H. Claus, B.W. Veal, R. Wheeler, A.P. Paulikas, and J.W. Downey, *Physica C* **193**, 243 (1992).
- [32] P. Gerdanian and C. Picard, *Physica C* **204**, 419 (1993).
- [33] W. Schwarz, O. Blaschko, G. Collin, and F. Marucco, *Phys.Rev. B* **48**, 6513 (1993).
- [34] A.A. Aligia, *Solid State Commun.* **78**, 739 (1991).
- [35] A.A. Aligia, *Europhys. Lett.* **26**, 153 (1994).
- [36] F. Yakhov, V. Plakhty, G. Uimin, P. Burlet, B. Kviatkovsky, J.Y. Henry, J.P. Lauriat, E. Elkaim, and E. Ressouche, *Solid State Commun.* **94**, 695 (1995).
- [37] P. Schleger, W.N. Hardy, and B.X. Yang, *Physica C* **176** 261 (1991); P. Schleger, W.N. Hardy, and H. Casalta, *Phys.Rev. B* **49**, 514 (1994).
- [38] M.A. Alario-Franco, C. Chaillout, J.J. Capponi, J. Chenavas, and M. Marezio, *Physica C* **156**, 455 (1988).
- [39] J. Reyes-Gasga, T. Krelels, G. van Tendeloo, J. van Landuyt, S. Amelinckx, X.H.M. Bruggink, and H. Verweij, *Physica C* **159**, 831 (1989).
- [40] Th. Zeiske, D. Hohlwein, R. Sonntag, F. Kubanek, and G. Collin, *Z.Phys. B* **86**, 11 (1992).
- [41] M. Schreckenberger and G. Uimin, *Sov.Phys. JETP Letters* **58**, 143 (1993).
- [42] G. Uimin and J. Rossat-Mignod, *Physica C* **199**, 251 (1992).
- [43] V.J. Emery, *Phys.Rev.Lett.* **58**, 2794 (1987).
- [44] A.A. Aligia and J. Garcés, *Phys. Rev.* **49**, 524 (1994).
- [45] P. Gawiec, D.R. Grempel, A.-C. Riiser, H. Haugerud, and G. Uimin, *Phys.Rev. B* **53**, 5872 (1996).
- [46] H. Haugerud, F. Ravndal, and G. Uimin, *J.Phys.: Condens. Matter* **5**, 6895 (1993).
- [47] C. Lanczos, *J. Res. Nat. Bur. Standards* **45**, 255 (1950).
- [48] P.A. Sterne and L.T. Wille, *Physica C* **162**, 223 (1989).
- [49] The metallic state is usually associated with orthorhombicity with an increased lattice constant in the chain direction. This reduces the hopping amplitude t and narrows the 1D band. The chemical potential counted from the 1D bottom determines the 1D band filling, decreasing with t , see Figure 12. The effective changes can be described by renormalizing the chemical potential and temperature.
- [50] J.B. Torrance, A. Benzinge, A.I. Nazzari, T.C. Huang, S.P. Parkin, D.T. Keane, S.J. LaPlaca, P.M. Horn, and G.A. Held, *Phys.Rev. B* **40**, 8872 (1989).
- [51] M.W. Shafer, T. Penney, B.L. Olson, R.L. Greene, and R.H. Koch, *Phys. Rev. B* **39**,

- 2914 (1989).
- [52] G. Baumgärtel, W. Hübner and K.H. Bennemann, Phys. Rev. B **45**, 308 (1992).
 - [53] L.D. Rotter, Z. Schlesinger, R.T. Collins, F. Holtzberg, C. Field, U.W. Welp, G.W. Crabtree, J.Z. Liu, Y. Fang, K.G. Vandervoort, and S. Fleshler, Phys. Rev. Lett. **67**, 2741 (1991).
 - [54] M.-H. Whangbo and C.C. Toradi, Science **249**, 1143 (1990).
 - [55] B.W. Veal and A.P. Paulikas, Physica C **184**, 321 (1991).

TABLES

Atom	Ion	Z	Radius
Ytterbium	Yb^{3+}	70	0.86
Yttrium	Y^{3+}	39	0.89
Neodymium	Nd^{3+}	60	0.995
Lanthanum	La^{3+}	57	1.02

TABLE I. Ionic radius in Å and atomic number Z of some trivalent rare earth ions RE^{3+} .

FIGURES

FIG. 1. Shown are two possible domains of the Ortho-I structure with orientations of chains along the horizontal (a) and vertical (b) axes; one of four domains of the Ortho-II structure (c); and a typical pattern of the tetragonal configuration with orientations of finite chain fragments along both x and y axes (d). Squares and filled (open) circles denote Cu atoms and O atoms (vacancies), respectively.

FIG. 2. Sketch of the ASYNNNI model, with interactions coupling oxygen atoms. Squares and filled (open) circles symbolize copper and oxygen atoms (vacancies).

FIG. 3. Schematic structural phase diagram of YBCO. Below the dashed curve, i.e. below T_R , equilibrium can hardly be reached experimentally.

FIG. 4. Examples of simple perfect structures consisting of the shortest CFs at $x = 0.5$, (a) and (b). The herringbone structure (a) would be favored by pure electrostatic (quadrupolar) interactions [41]. Squares and filled (open) circles denote copper and oxygen atoms (vacancies).

FIG. 5. Free energy per oxygen atom, f , of Cu-O chains versus chain length (or number of oxygen atoms), n , for various values of U_{end} at $T = 0.06 \approx 900$ K. For each curve, the chemical potential has been chosen so that the concentration of oxygen holes is 0.3 for the longest chains, independent of U_{end} . The free energy is measured in units of the hopping parameter $t \approx 15000$ K.

FIG. 6. Free energy per oxygen atom, f , of Cu-O chains versus length, n , for equidistant values of the chemical potential, ranging from 1.5 to 2.0, at $U_{\text{end}} = 1.0$ and $T = 900$ K.

FIG. 7. Free energy per oxygen atom, f , of Cu-O chains vs length, n , for a few temperatures, with $U_{\text{end}} = 1.0$ and the hole concentration being 0.3 for the longest chains. Open symbols denote fits to expression (5).

FIG. 8. V_2 vs temperature, T , for a set of equidistant values of U_{end} . The hole oxygen hole concentration is taken to be 0.3 for the longest, $n = 6$, chains.

FIG. 9. \tilde{V}_2 vs temperature, T , for a set of equidistant values of U_{end} . The oxygen hole concentration is 0.3 for the longest chains.

FIG. 10. Ortho-II order parameter, m_{II} , vs U_{end} , at $T_{\text{II}} = 0.03$ corresponding to 450 K. The full symbols denote Monte Carlo data for the extended ASYNNNI model, applied to YBCO; the interpolating line is included as a guide to the eye.

FIG. 11. V_2 (full symbols) and \tilde{V}_2 (open symbols) vs chemical potential μ for various temperatures, at $U_{\text{end}} = 1.02$.

FIG. 12. Illustration of shifting of bands by going from the semiconducting (tetragonal) to the metallic (orthorhombic) state in REBCO compounds. The 1D hole band filling is larger in the semiconducting state.

FIG. 13. Phase diagram (temperature $T(K)$ in Kelvin vs. oxygen content x) obtained from MC simulations of the extended ASYNNNI model for YBCO. Typically, systems with 40×40 copper ions were considered.

FIG. 14. Concentration of twofold coordinated Cu ions, c_2 , versus oxygen content, x , at various temperatures. Simulations of the extended ASYNNNI model for YBCO were done at $T = 300$ K and 600 K. MC data are shown by full dots; interpolating lines are included, for clarity, as guides to the eye. Experimental results [3,4] are denoted by open symbols.

FIG. 15. Concentration of two-, three- and fourfold coordinated Cu ions, c_l ($l=2,3$, and 4) versus oxygen content, x , at $T = 450$ K, simulating the extended ASYNNNI model for YBCO, $\mu = 1.59$ (full symbols and, as guide to the eye, lines). For comparison, experimental data [1] are shown (open symbols).

FIG. 16. Notation as in Figure 15; however, in this case for NdBCO, taking the chemical potential μ to be 1.62.

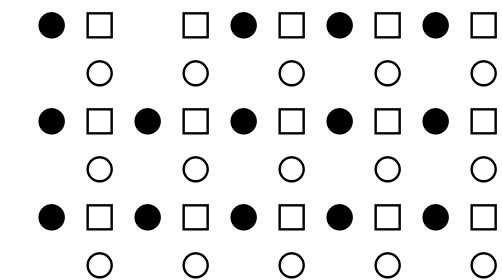
FIG. 17. Notation as in Figure 15; however, in this case for LaBCO, taking the chemical potential μ to be 1.66.

FIG. 18. Number of holes per oxygen atom, $\overline{\nu_h(n)}/n$, leaving a CF of length n ($n = 2, \dots, 6$), as function of temperature T , at $\mu = 1.59$ ($\nu_h = 0$ for $n = 1$).

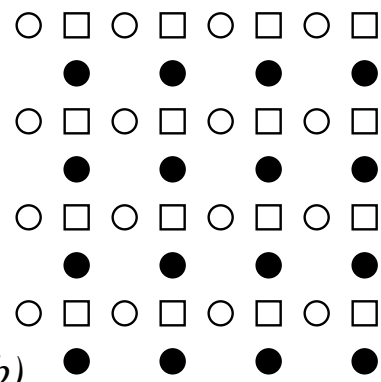
FIG. 19. Charge transfer, n_h , as function of oxygen content x , at various temperatures from 300 K to 600 K, simulating the extended ASYNNNI model for YBCO.

FIG. 20. Charge transfer, n_h , as function of oxygen content, x , simulating the extended ASYNNNI model mimicing RE= La, Nd, Y and Yb (from bottom to top).

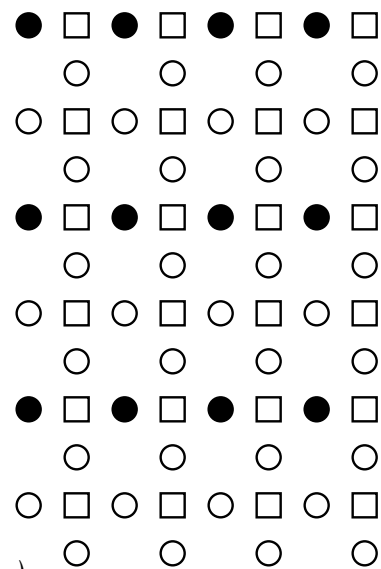
FIG. 21. Average chain length, ℓ , as function of oxygen content, x , simulating the extended ASYNNNI model mimicing RE= La, Nd, and Y (from bottom to top). Full and open symbols denote direct and indirect (through c_3) determination of ℓ , respectively; see text.



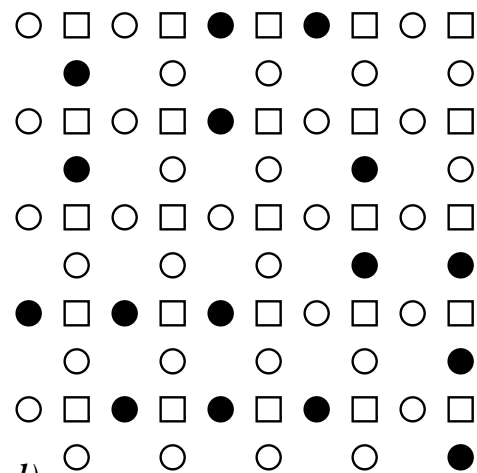
a)



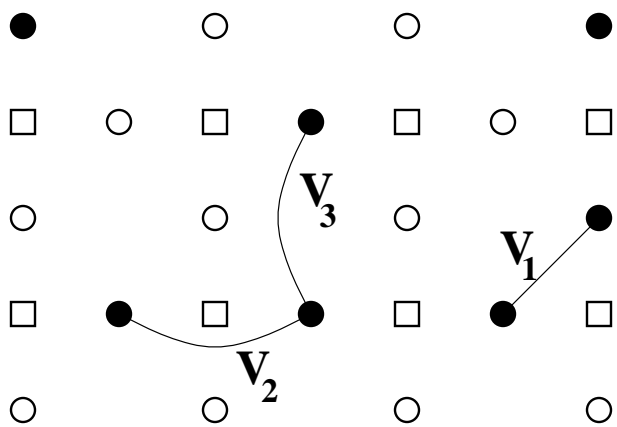
b)

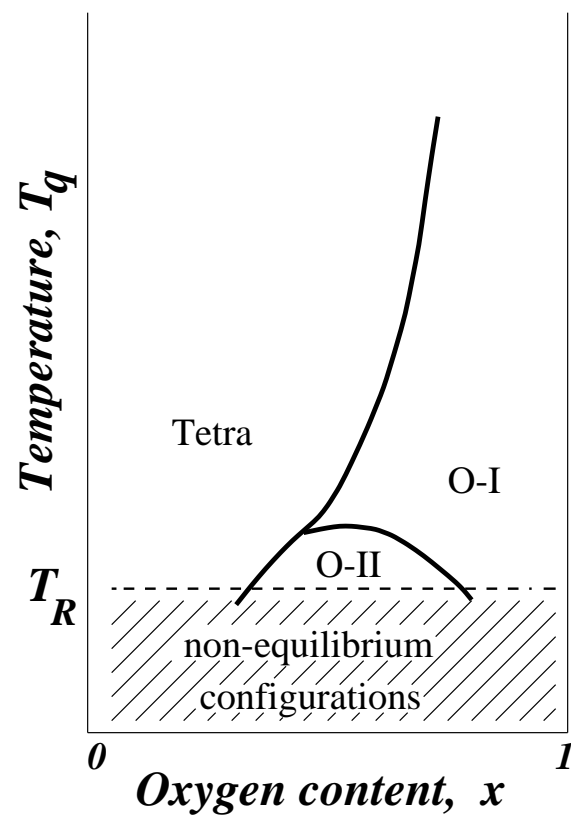


c)

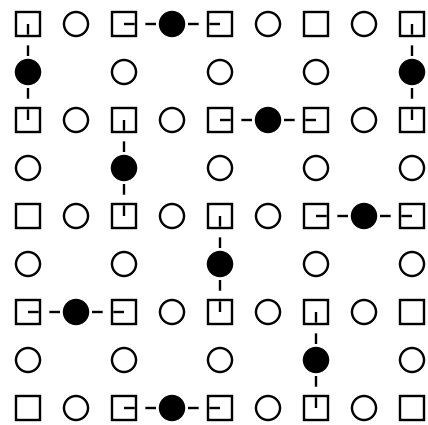


d)





a)



b)

